Effects of Diabetes on Mitochondrial Morphology and Its Implications in Diabetic Retinopathy

Dongjoon Kim[1,2] and Sayon Roy[1,2]

[1]Department of Medicine, Boston University School of Medicine, Boston, Massachusetts, United States
[2]Department of Ophthalmology, Boston University School of Medicine, Boston, Massachusetts, United States

Correspondence: Sayon Roy, Departments of Medicine and Ophthalmology, Boston University School of Medicine, 650 Albany Street, Boston, MA 02118, USA; sayon@bu.edu.

Received: February 4, 2020
Accepted: June 15, 2020
Published: August 5, 2020

Citation: Kim D, Roy S. Effects of diabetes on mitochondrial morphology and its implications in diabetic retinopathy. *Invest Ophthalmol Vis Sci.* 2020;61(10):10. https://doi.org/10.1167/iovs.61.10.10

Purpose. To determine whether high glucose (HG) or diabetes alters mitochondrial morphology and promotes mitochondrial fragmentation in retinal vascular cells and thereby triggers apoptosis associated with diabetic retinopathy.

Methods. To assess whether diabetes promotes mitochondrial fragmentation and thereby triggers apoptosis, retinas from nondiabetic and diabetic rats were analyzed using electron microscopy (EM) and in parallel, wild-type, diabetic, and OPA1$^{+/-}$ mice were analyzed for optic atrophy gene 1 (OPA1) and cytochrome c levels using Western blot (WB) analysis. To assess the relationship between mitochondrial fragmentation and OPA1 levels, rat retinal endothelial cells (RRECs) were grown in normal (N; 5 mmol/L) medium, HG (30 mmol/L) medium, or in N medium transfected with OPA1 siRNA for seven days. Cells were examined for OPA1 expression and cytochrome c release by WB. In parallel, cells were stained with MitoTracker Red and assessed for mitochondrial fragmentation in live cells using confocal microscopy.

Results. EM images revealed significant mitochondrial fragmentation in vascular cells of retinal capillaries of diabetic rats compared with that of nondiabetic rats. WB analysis showed significant OPA1 downregulation concomitant with increased levels of proapoptotic cytochrome c levels in cells grown in HG and in cells transfected with OPA1 siRNA alone. Similarly, OPA1 level was significantly reduced in diabetic retinas compared with that of nondiabetic retinas. Interestingly, OPA1$^{+/-}$ animals exhibited elevated cytochrome c release similar to those of diabetic mice.

Conclusions. Findings indicate that diabetes promotes mitochondrial fragmentation in retinal vascular cells, which are driven, at least in part, by decreased OPA1 levels leading to apoptosis in diabetic retinopathy.

Keywords: electron microscopy, mitochondria, high glucose, diabetes, retinal endothelial cells

Diabetic retinopathy, the leading cause of blindness in the working age population,[1,2] is characterized by early vascular lesions involving apoptotic cell death.[3–8] Our previous studies suggest that mitochondrial fragmentation contributes to accelerated apoptotic cell loss associated with diabetic retinopathy.[9–15] Although high glucose (HG) triggers mitochondrial fragmentation in retinal endothelial cells and pericytes in vitro,[10,11] it is unclear whether this phenomenon occurs in vivo during the development and progression of diabetic retinopathy. To determine whether such morphologic changes involving mitochondrial fragmentation develops in diabetic retinas, in this study, we have examined vascular cells in the retinal capillaries from nondiabetic and diabetic rats using transmission electron microscopy. Furthermore, to gain mechanistic insights into how such mitochondrial fragmentation develops, we investigated to what extent optic atrophy gene 1 (OPA1), a mitochondrial fusion protein, plays a role in the retinas of diabetic animals.

Maintenance of mitochondrial structure is regulated through a delicate balance between fission and fusion events. OPA1 is a fusion gene that plays a key role in preserving mitochondrial morphology and the mitochondrial network.[16–19] OPA1, a dynamin-related GTPase, is associated with the inner mitochondrial membrane where it mediates inner membrane fusion[20] and acts as a gatekeeper of cytochrome c release during apoptosis.[21] After its biogenesis, proteolytic cleavage of the OPA1 protein results in a long and a short form of OPA1. The long form of OPA1 is present as an integral membrane protein on the mitochondrial inner membrane whereas the short form of OPA1 resides in the mitochondrial intermembrane space.[22] In the absence of OPA1, there could be partial mitochondrial fusion, but the process would be incomplete and may lead to mitochondrial fragmentation even in the presence of outer membrane fusion proteins.[23] This suggests that OPA1 is functionally required for successful mitochondrial fusion[24] and that compromised OPA1 function could thereby lead to mitochondrial fragmentation. It is important to note that in addition to OPA1, which facilitates fusion of the inner mitochondrial membrane, MFN1 and MFN2, outer mitochondrial membrane proteins of the dynamin family, tethers apposing

mitochondria to promote fusion of the outer mitochondrial membrane.[25,26]

The importance of OPA1 has been underscored through various studies with regard to maintenance of mitochondrial morphology.[27–36] Deficiency of OPA1 has been shown to contribute to mitochondrial fragmentation in various cell types, including HeLa cells,[27] mouse coronary endothelial cells,[29] human ovarian carcinoma cell line,[19] and mouse embryonic fibroblasts.[18] Reduced OPA1 levels in a muscle-specific OPA1 knockout model not only disrupted mitochondrial structure but also progressively impaired mitochondrial respiratory capacity by reducing oxygen consumption rates,[31] leading to dysfunctional mitochondria and subsequent apoptotic cell death.[32] These studies implicate OPA1 deficiency as a potential contributory factor underlying mitochondrial fragmentation in apoptotic cell loss associated with diabetic retinopathy.

To verify whether HG–induced mitochondrial fragmentation seen in retinal vascular cells in vitro also develops in vivo, electron micrographs of retinal tissues from nondiabetic and diabetic rats were examined. To determine the role of OPA1 in mitochondrial dysfunction, in the present study, we examined whether HG condition alters OPA1 expression, promotes mitochondrial fragmentation, and triggers cytochrome c release in vitro. In addition, studies were conducted to assess whether OPA1 levels were altered in the diabetic retinas, and whether decreased levels of OPA1 result in elevated cytochrome c levels using an OPA1$^{+/-}$ animal model.

Methods

Cell Culture

Rat retinal capillary endothelial cells (RRECs) that were positive for von Willebrand factor (vWF) were used in this study and were isolated as previously described.[37] To investigate the effect of abnormal OPA1 downregulation and cytochrome c release, RRECs were grown in normal (N, 5 mmol/L glucose), HG (25 or 30 mmol/L glucose) Dulbecco's modified Eagle medium (DMEM) containing 10% fetal bovine serum (Sigma, St. Louis, MO, USA), antibiotics and antimycotics for seven days. In parallel, cells grown in N medium were exposed to 25 or 30 mmol/L mannitol as osmotic control. Cells grown according to the experimental groups were then assessed for OPA1 expression, cytochrome c release, and mitochondrial morphology.

Animals

Animal studies were conducted following the ARVO Statement for the Use of Animals in Ophthalmic and Vision Research. Twelve Sprague-Dawley rats were used to assess mitochondrial morphology changes in diabetic retinas. Additionally, 12 wild-type (WT) C57/BL6 mice (Harlan Lab, Inc, Indianapolis, IN, USA) and six OPA1$^{+/-}$ mice bred into the C57/BL6 background kindly provided by Dr. Marcella Votruba[17] were used in the study. Genotypes of the mice were determined by polymerase chain reaction (PCR) at weaning using tail tip DNA and then again at sacrifice. PCR reactions were prepared using the PCR enzyme solution (PCR Master Mix; Promega, Madison, WI, USA) along with the following primers: Primer 1, 5′–CTCTTCATGTATCTGTGGTC–3′; Primer 2, 5′–TTACCCGTGGTAGGTGATCATG–3′; Primer 3, 5′–TTACCCGTGGTAGGTGATCATA–3′. Primers 1 and 2 amplify an approximately 160-bp fragment from the WT OPA1 allele. Primers 1 and 3 amplify a 160-bp fragment from the OPA1$^{+/-}$ allele. The OPA1$^{-/-}$ genotype was not used in this study as it is known to cause perinatal lethality.[17]

Streptozotocin (STZ) was injected intraperitoneally (55 mg/kg body weight) in six WT mice to induce diabetes. Blood and urine glucose concentrations were monitored two or three days after STZ injection to confirm onset of diabetes in the animals. The remaining six WT and six OPA1$^{+/-}$ mice served as nondiabetic controls. In parallel, to assess diabetes-induced changes in mitochondrial morphology, electron micrographs of six nondiabetic and six diabetic rat retinas were analyzed. Blood glucose levels were measured in each animal two to three times weekly and at the time of death. Mice or rats exhibiting blood glucose levels of ~350 mg/dL represented were included as the diabetic group. Neutral protamine hagedorn (NPH) insulin was administered to diabetic animals as needed to maintain blood glucose levels ~350 mg/dL. After 16 weeks of diabetes, animals from all experimental groups were killed, retinas isolated, and total protein obtained. To determine the effect of diabetes on OPA1 and cytochrome c expression, protein isolated from diabetic mouse retinas and nondiabetic mouse retinas were subjected to WB analysis.

Cell Transfection with OPA1 Small Interfering RNA (siRNA) and Isolation of Cytosolic and Mitochondrial Fractions

To investigate the effect of reduced OPA1 expression on cytochrome c release and mitochondrial morphology, RRECs were grown in N medium and transfected with 100 µmol/L OPA1 siRNA (Invitrogen, Carlsbad, CA, USA) in the presence of 8 µmol/L Lipofectin (Invitrogen). To isolate mitochondrial and cytosolic fractions from cell lysates, cells grown in N medium, HG medium, or N medium transfected with OPA1 siRNA were washed with phosphate-buffered saline solution and underwent lysis using 0.1% Triton-X-100 buffer that contains 10 mmol/L Tris, pH 7.5, 1 mmol/L ethylenediamine tetra-acetic acid, and 1 mmol/L phenylmethylsulfonyl fluoride. The cell lysate was then spun in a centrifuge at 700*g* for 5 minutes. After centrifugation, the supernatant was taken and spun in a centrifuge again at 21,000*g* for 15 minutes, and the resultant supernatant was isolated as the cytosolic fraction. The residual cellular pellet was subjected to washes with the Triton buffer previously described and underwent centrifugation at 21,000*g* for 15 minutes. The supernatant was carefully removed and thrown away while the remaining cellular pellet was washed with radioimmunoprecipitation assay buffer that contained 1 mmol/L phenylmethylsulfonyl fluoride, followed by centrifugation at 21,000*g* for 15 minutes. The resultant supernatant was isolated as the mitochondrial fraction. The mitochondrial and cytosolic fractions of cell lysates were then subjected to WB analysis to determine cytochrome c release. In addition, cytosolic and mitochondrial fractions were obtained from retinas of WT mice, diabetic mice, and OPA1$^{+/-}$ mice using the Mitochondria Isolation Kit (Thermo Scientific, Waltham, MA, USA) designed for intact mitochondrial isolation from tissues. The mitochondrial and cytosolic fractions from retinal tissues were then subjected to WB analysis to assess cytochrome c levels.

Investigative Ophthalmology & Visual Science

Western Blot Analysis

To assess OPA1 expression and cytochrome c release, cytosolic and mitochondrial fractions of RRECs from the experimental groups were subjected to WB analysis. In parallel, protein samples isolated from diabetic or nondiabetic mouse retinas were subjected to WB analysis to examine OPA1 and cytochrome c levels. Bicinchoninic acid protein assay (Pierce Chemical, Rockford, IL) was used to obtain protein concentrations of cell lysates and retinal tissues. A 10% SDS-polyacrylamide gel was loaded with equal amount of protein (20 µg) in separate lanes and electrophoresed along with a molecular weight marker (Lonza, Basel, Switzerland). After completion of electrophoresis, protein was then transferred onto a PVDF membrane (Millipore, Billerica, MA, USA) using a semidry apparatus according to Towbin's procedure.[38] The membrane was blocked with 5% nonfat dry milk for two hours and incubated overnight at 4°C with mouse monoclonal OPA1 antibody (1:2500, Catalog no. 612606; BD Biosciences, San Jose, CA, USA) or mouse monoclonal cytochrome C antibody (1:500, Catalog no. ab13575; Abcam, Cambridge, MA, USA) solution in Tris-buffered saline solution containing 0.1% Tween-20 (TTBS) and 5% bovine serum albumin. Next day, the membrane was subjected to TTBS washes and exposed to a secondary antibody solution containing anti-rabbit IgG, AP-conjugated antibody (1:3000, Catalog no. 7054; Cell Signaling, Danvers, MA, USA) or anti-mouse IgG, AP-conjugated antibody (1:3000, Catalog no. 7056, Cell Signaling) in room temperature for one hour. Immun-Star chemiluminescent substrate (Bio-Rad, Hercules, CA, USA) was used on the membrane after TTBS washes, and chemiluminescent signals were captured using the LAS-4000 digital imaging system (Fujifilm, Tokyo, Japan). Equal loading of protein samples was ascertained by Ponceau-S staining after transfer, and by β-actin antibody (1:1000, Catalog no. 4967, Cell Signaling) or VDAC1 antibody (1:1000, Catalog no. sc-390996; Santa Cruz Biotechnology, Dallas, TX, USA). To determine OPA1, cytochrome C, VDAC1, and β-actin protein expression, chemiluminescent signals were subjected to densitometric analysis at non-saturating thresholds by Image J software (developed by Wayne Rasband, National Institutes of Health, Bethesda, MD, USA).

Live Confocal Microscopy and Analysis of Mitochondrial Morphology

Cells from experimental groups grown on poly-D-lysine-coated glass slide-bottom dishes (MatTek) were stained by MitoTracker Red, maintained at 37°C in a 5% CO_2 humidified microscope stage chamber and were imaged live via confocal microscopy to capture mitochondrial morphology using a Zeiss LSM 710 Meta microscope (Carl Zeiss, Oberkochen, Germany) with a 63× oil immersion objective. MitoTracker Red was subjected to 543 nm helium/neon laser excitation, and emission was recorded through a bandpass 650 to 710 nm filter (Zeiss, Thornwood, NY, USA). Captured images of mitochondria were quantitatively analyzed for changes in mitochondrial morphology by assessing values of form factor (FF) and aspect ratio (AR) values.[39,40] In ImageJ, mitochondria images underwent processing with a median filter to attain equal fluorescent pixels. Then, particle analysis was performed on images of mitochondria to obtain values of FF (4^*Area/perimeter^2) and AR (length of major axis divided by length of minor axis). A value of 1 for FF corresponds to a circular, unbranched mitochondrion while higher values of FF represent a longer mitochondrion with increased extent of branching. A value of 1 for AR represents a perfect circle, whereas higher values of AR indicate a higher extent of mitochondrial elongation. At least ten random fields from live confocal microscopy were taken in each experimental group and were subjected to AR and FF quantitative analysis.

Electron Microscopy

Eyes from nondiabetic or diabetic rats were enucleated, and retinas isolated were fixed in 2.5% glutaraldehyde in a 0.1 mol/L cacodylate buffer. Osmium tetraoxide, ethanol, and propylene oxide (EMS, Hatfield, PA, USA) were used to dehydrate the tissues, which were then embedded in an Epon-Araldite plastic mixture and baked for 48 hours. After the embedding procedure, ultrathin sections were sliced serially at 60 to 70 nm using a microtome (LKB Ultratome Nova, Bromma, Sweden). Subsequently, the sections were placed on a copper grid, stained with 4% uranyl acetate in methanol, and images were acquired using a transmission electron microscope (Philips, Electron Optics, Eindhoven, Netherlands). Electron micrographs were taken of retinal capillaries spanning the outer plexiform and ganglion cell layers and analyzed for mitochondrial morphology. Electron microscopy images were analyzed for a total number of mitochondria per section from nondiabetic and diabetic animals. Fragmented mitochondria per section were scored from each of these images from nondiabetic animals and compared with those of diabetic animals.

Statistical Analysis

Data from this study are reported as mean ± standard deviation. Data from the control group were normalized to 100% while data from other experimental groups were indicated as percentages of control. Comparison between two groups was performed using a Student *t*-test. Comparisons among three or more groups were performed using one-way analysis of variance followed by Bonferroni's post-hoc test. Data with $P < 0.05$ was considered significant.

Results

Mitochondrial Fragmentation in Vascular Cells of Retinal Capillaries in Diabetic Rats

A total of 38 images (n = 8) representing nondiabetic animals were analyzed for fragmented mitochondria in the retinal capillaries and compared to those of diabetic animals. A fivefold increase in the number of fragmented mitochondria was observed in the vascular cells of retinal capillaries in diabetic animals compared with those of nondiabetic animals ($P < 0.001$; Fig. 1).

HG Downregulates OPA1 Expression in RRECS

RRECs grown in 25 mmol/L HG medium (74.3 ± 4.1% of N; $P < 0.01$; Figs. 2A, 2B) or 30 mmol/L HG medium (69.7 ± 5.9% of N; $P < 0.01$; Figs. 2A, 2B). had significantly reduced OPA1 compared with cells grown in N medium. In addition, cells grown in 25 mmol/L mannitol (100.3 ± 4.0% of N; $P > 0.05$; Figs. 2A, 2B) or 30 mmol/L mannitol (95.5 ± 0.11% of N; $P > 0.05$; Figs. 2A, 2B) used as osmotic control showed no significant difference in OPA1 expression

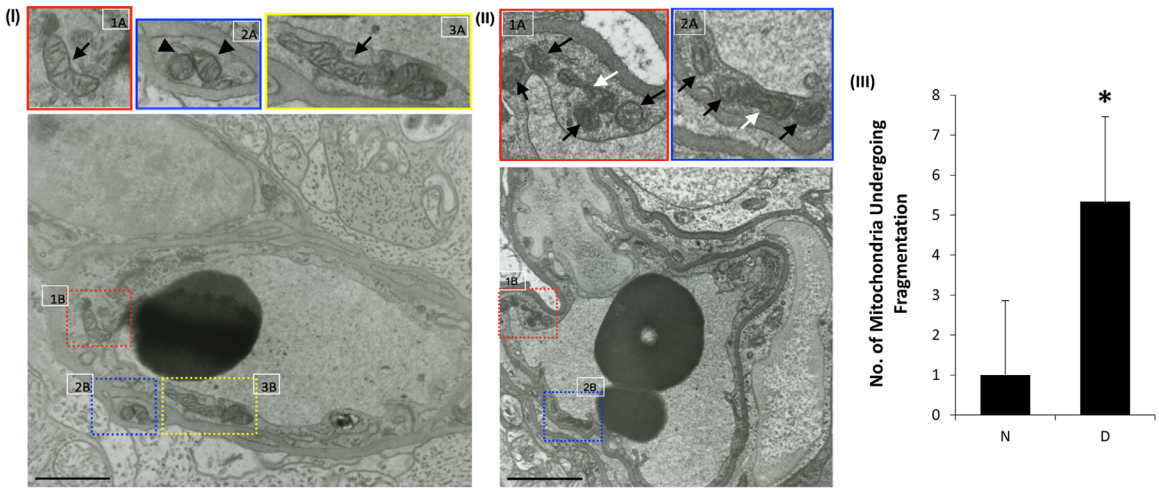

Figure 1. EMs show mitochondrial morphology change in retinal vascular cells of diabetic rats. (**I**) Intact, elongated, tubular mitochondria in vascular cells of non-diabetic rat retinas. (**II**) Fragmented mitochondria (black arrows) or mitochondria undergoing fragmentation (white arrows) in the diabetic rat retinas. Fragmented mitochondria are frequently seen in the diabetic retinas. *Left panel:* insets at the top (**1A, 2A, 3A**) show enlarged views of corresponding areas from lower panel (**1B, 2B, 3B**). Note: enlarged view shows tubular structure and cristae in the mitochondrion. *Right panel:* insets at the top (**1A, 2A**) show enlarged views of corresponding areas from lower panel (**1B, 2B**). *Scale bar:* 1 µm. (**III**) Graph of cumulative data indicate that diabetic (*D*) retinas exhibit a fivefold increase in the number of mitochondria undergoing fragmentation compared to that of nondiabetic (*N*) retinas. $^{*}P < 0.001$ versus *N*, n = 6.

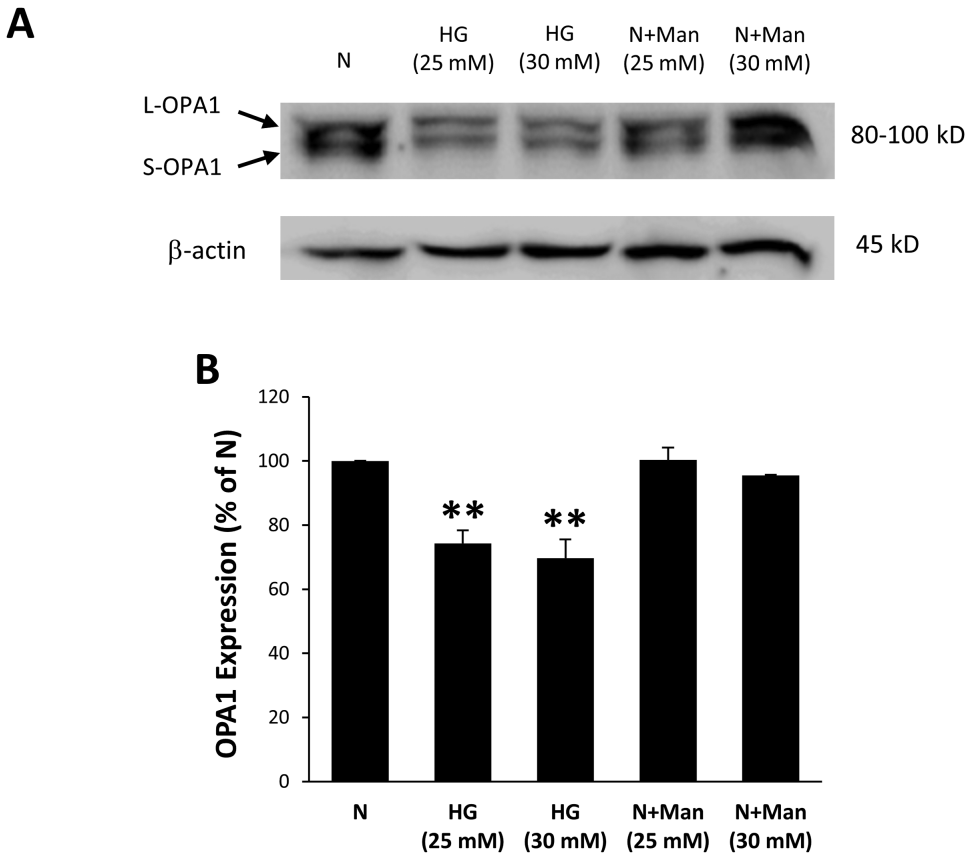

Figure 2. Effects of HG on OPA1 expression in RRECs. (**A**) Representative WB image shows OPA1 is downregulated in cells grown in 25 mmol/L or 30 mmol/L HG. Cells exposed to 25 mmol/L or 30 mmol/L mannitol (*Man*) show no significant difference in OPA1 expression compared to cells grown in N medium. (**B**) Graphical illustration of cumulative data shows 25 mmol/L or 30 mmol/L HG significantly downregulates OPA1 expression. Data are expressed as mean ± SD. $^{**}P < 0.01$ versus N, n = 6.

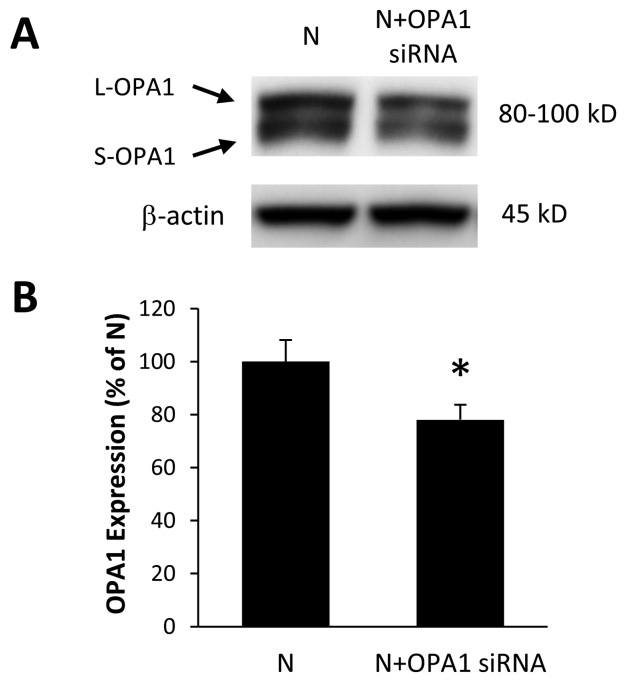

Figure 3. OPA1 downregulation using OPA1 siRNA. (**A**) Representative WB image shows OPA1 siRNA successfully leads to OPA1 downregulation compared to that of cells grown in normal (*N*) medium. (**B**) A graph of cumulative data indicate that cells transfected with OPA1 siRNA exhibit a significant decrease in OPA1 expression compared to cells grown in N medium. $^{*}P < 0.05$ versus N, n = 6.

compared with cells grown in N medium alone. In addition, cells transfected with OPA1 siRNA showed OPA1 downregulation as expected compared with cells grown in N medium alone (78.0 ± 10.2% of N; $P < 0.05$; Figs. 3A, 3B).

OPA1 Downregulation Promotes Mitochondrial Fragmentation in RRECs

Live mitochondrial imaging data using confocal microscopy indicated that the cells grown in 25 mmol/L HG medium and 30 mmol/L HG medium showed significant reduction in values of FF and AR compared to those grown in N medium (N: FF = 4.07 ± 0.54. AR = 2.42 ± 0.13; 25 mmol/L HG: FF = 2.39 ± 0.34; $P < 0.01$. AR = 1.89 ± 0.09; $P < 0.05$; 30 mmol/L HG: FF = 2.39 ± 0.32; $P < 0.01$; AR = 1.91 ± 0.11; $P < 0.05$; Figs. 4A, 4B). Cells exposed to 25 or 30 mmol/L mannitol (25 mmol/L mannitol: FF = 3.56 ± 0.14; $P > 0.05$. AR = 2.33 ± 0.20; $P > 0.05$; 30 mmol/L mannitol: FF = 3.86 ± 0.51; $P > 0.05$; AR = 2.34 ± 0.23; $P > 0.05$, Figs. 4A, 4B) used as osmotic controls showed no significant difference in FF or AR values compared with those of cells grown in N medium. Interestingly, cells grown in N medium and transfected with OPA1 siRNA showed significant reduction in FF and AR values (N+OPA1 siRNA: FF = 2.54 ± 0.11; $P < 0.01$; AR = 1.92 ± 0.05; $P < 0.05$, Figs. 4A, 4B) similar to cells grown in HG medium.

Effects of HG and OPA1 Downregulation On Cytochrome C Release in RRECs

WB results indicated that cells grown in HG medium exhibited a significant increase in cytochrome c release (264.0 ± 28.1% of N; $P < 0.05$; Figs. 5A, 5B) compared that of cells grown in N medium. Interestingly, cells grown in N medium and transfected with OPA1 siRNA alone also exhibited a significant increase in cytochrome c release (231.5 ± 26.8% of N; $P < 0.05$; Figs. 5A, 5B) similar to that of cells grown in HG medium.

Diabetes Downregulates OPA1 Expression and Promotes Apoptosis in Mouse Retinas

WB data revealed significant OPA1 downregulation in diabetic mouse retinas compared that of non-diabetic wild-type mouse retinas (48.6% ± 2.9% of N; $P < 0.01$; Figs. 6A, 6C). As expected, $OPA1^{+/-}$ mouse retinas showed reduced OPA1 expression compared wild-type mouse retinas (51.3% ± 3.7% of N; $P < 0.01$; Figs. 6A, 6C). Additionally, diabetic mouse retinas exhibited elevated cytochrome c release compared that of nondiabetic wild-type mouse retinas (216% ± 13.4% of N; $P < 0.01$; Figs. 6B, 6D). Interestingly, $OPA1^{+/-}$ mouse retinas had similar elevation in cytochrome c release compared with that of nondiabetic wild-type mouse retinas (184% ± 15.1% of N; $P < 0.01$; Figs. 6B, 6D).

Discussion

The present study demonstrates for the first time that mitochondrial fragmentation develops in vascular cells of diabetic retinal capillaries associated with decreased OPA1 expression in the retinas of diabetic animals. Additionally, we observed in vitro that HG-induced downregulation of OPA1 expression in RRECs results in cytochrome c release and mitochondrial fragmentation. Interestingly, reducing OPA1 expression alone using OPA1 siRNA yielded similar findings. The 25 and 30 mmol/L glucose concentrations showed no significant difference in OPA1 expression levels or extent of mitochondrial fragmentation. In addition, mannitol used as osmotic control showed no significant change in OPA1 expression or extent of mitochondrial fragmentation compared to cells grown in normal condition. Importantly, we observed OPA1 downregulation together with increased cytochrome c levels in the diabetic retinas. These results indicate that reduced OPA1 levels may contribute to mitochondrial fragmentation and increase in cytochrome c level in $OPA1^{+/-}$ mice, suggesting that OPA1 plays a significant role in regulating mitochondrial dynamics and maintenance of cell survival.

Recent studies have shed light on OPA1 and its relationship to apoptosis. Reduced OPA1 levels were shown to block mitochondrial fusion, promote mitochondrial fragmentation, and lead to cytochrome c release, which in turn, triggers apoptosis. This specific pathway was verified in studies using siRNA-mediated OPA1 downregulation leading to mitochondrial fragmentation and the release of cytochrome c.[16,19] Another study reported that in diabetic mice, the OPA1 level is significantly decreased in coronary endothelial cells concomitant with increased mitochondrial fragmentation seen in diabetes.[29] These findings suggest that reduced OPA1 expression tilts the balance between fusion and fission events favoring fission and that such changes result in mitochondrial fragmentation, cytochrome c release, triggering caspase-dependent apoptosis. While cytochrome c release ultimately leads to activation of caspase-3 and promotes apoptosis,[41] activated caspase-3 has also been

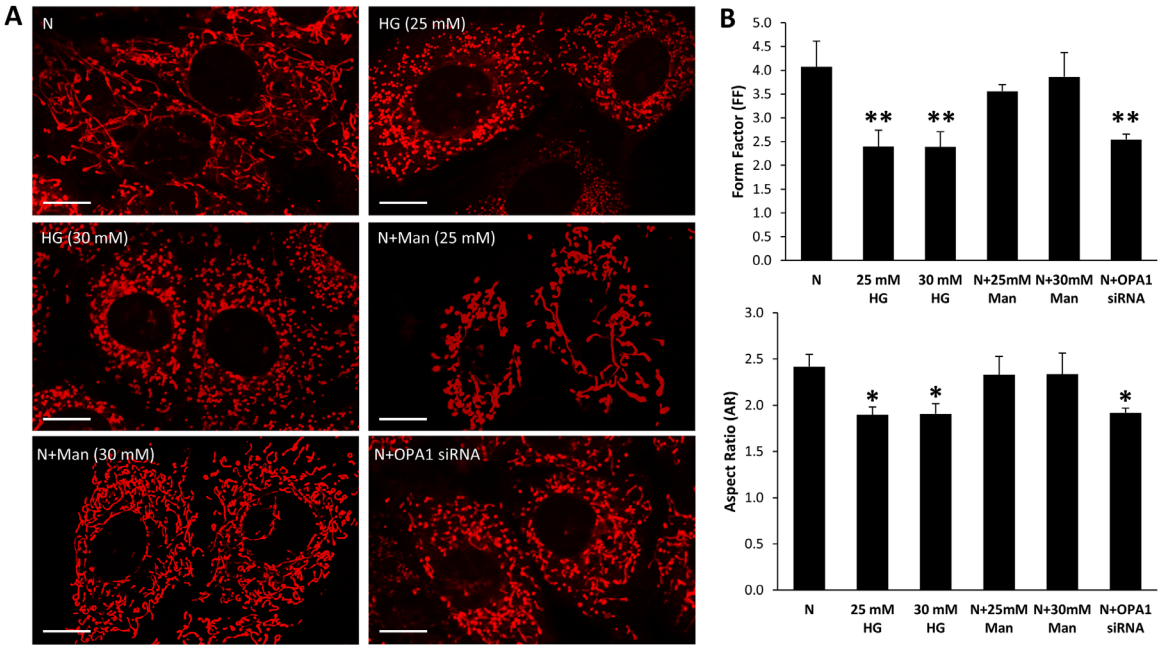

Figure 4. OPA1 downregulation compromises mitochondrial morphology and promotes mitochondrial fragmentation. (**A**) Representative confocal images of RRECs grown in normal (*N*) medium stained with mitotracker red show long, tubular networks of mitochondria. Cells grown in 25 mmol/L or 30 mmol/L mannitol (*Man*) showed no significant difference in mitochondrial morphology compared with that of cells grown in N medium. In parallel, cells grown in 25 mmol/L or 30 mmol/L high glucose (*HG*) medium (*middle panel*) and cells transfected with OPA1 siRNA (*right panel*) exhibit significant mitochondrial fragmentation. *Scale bars:* 10 µm. (**B**) A graph of cumulative data indicates that cells grown in HG medium and cells transfected with OPA1 siRNA exhibit a significant decrease in FF and AR values compared with cells grown in N medium. $^{**}P < 0.01$; $^{*}P < 0.05$, n = 6.

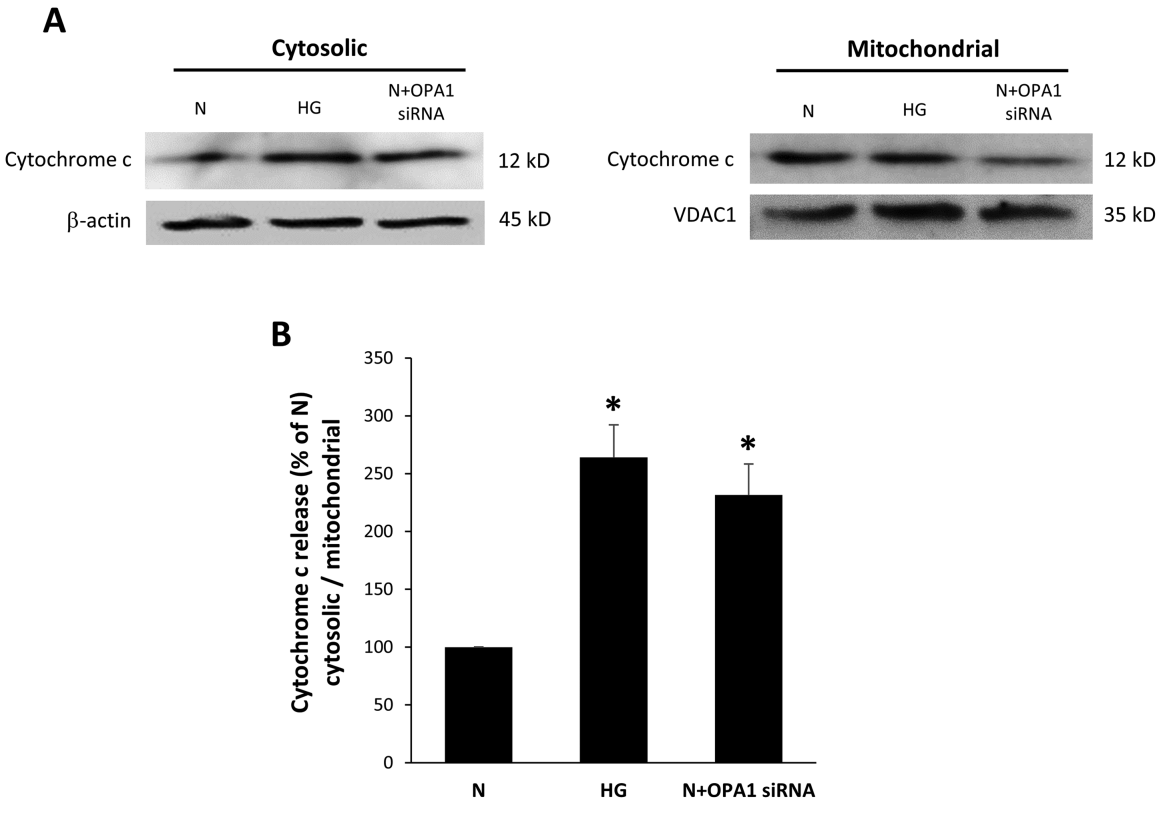

Figure 5. Effects of HG and OPA1 downregulation on cytochrome c release in RRECs. (**A**) Representative WB image demonstrates increased cytochrome c release in cells grown in HG and in cells transfected with OPA1 siRNA. (**B**) Graphical illustration of cumulative data shows HG or OPA1 siRNA significantly promotes cytochrome c release in cells grown in HG and in cells transfected with OPA1 siRNA. Data are expressed as mean ± SD. $^{*}P < 0.05$ vs N, n = 6.

Investigative Ophthalmology & Visual Science

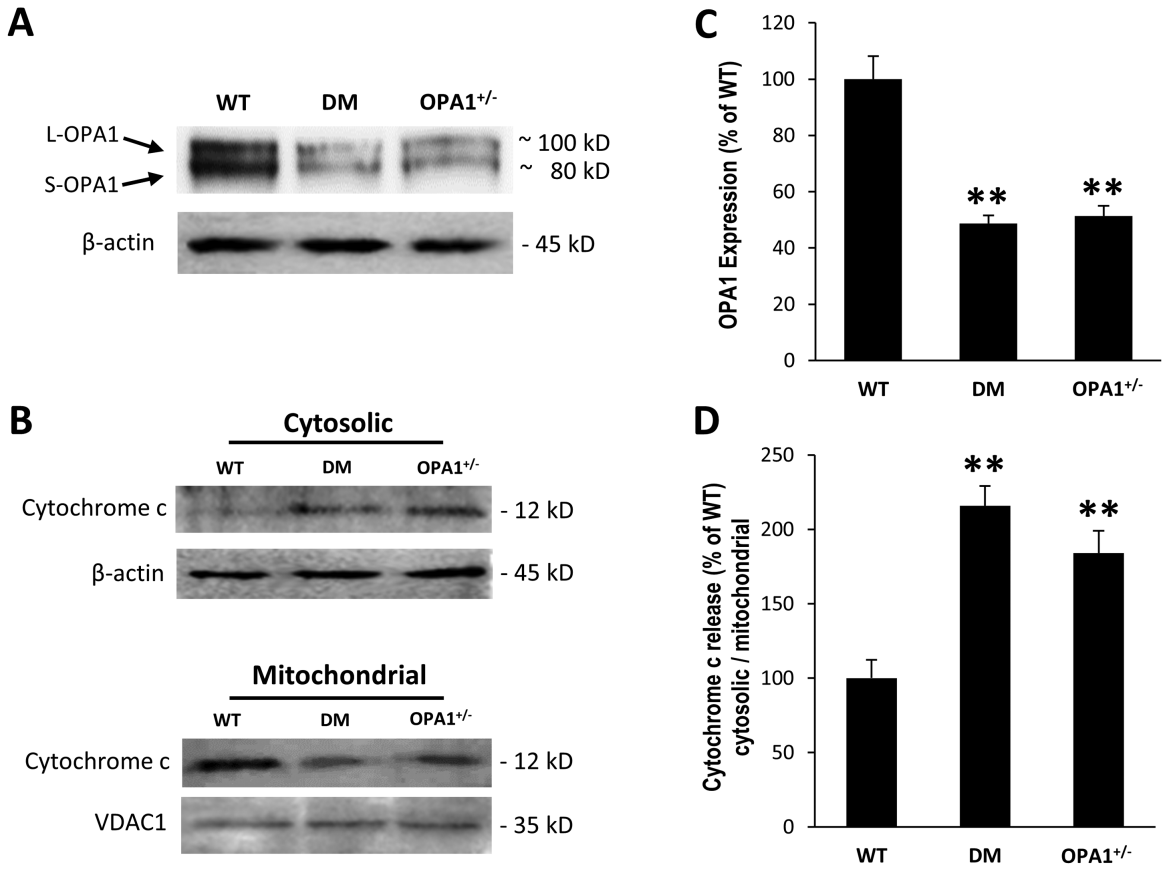

Figure 6. OPA1 downregulation promotes cytochrome c release in mouse retinas. (**A**) Representative WB image shows OPA1 is downregulated in retinas of diabetic mice and in retinas of OPA1$^{+/-}$ mice. (**B**) Representative WB images show increased cytochrome c release in retinas of diabetic and OPA1$^{+/-}$ mice compared with those of WT mice. Graphical illustration of cumulative data shows (**C**) OPA1 downregulation is associated with an increase in (**D**) cytochrome c release. Data are expressed as mean ± SD. $^{**}P < 0.01$ versus WT, n = 6.

reported to participate in nonapoptotic cellular responses such as remodeling of actin cytoskeleton[42] and macrophage polarity formation.[43] Additionally, studies have shown a functional correlation with OPA1 depletion and mitochondrial function. Mice with deficient OPA1 exhibited decreased copy number of mtDNA and reduced levels of nuclear antioxidant genes.[44] Additionally, decreased activities of complexes I and IV were found in the hearts of OPA1$^{+/-}$ mice.[44] These observations indicate that maintenance of mitochondrial respiration and energy production is partly regulated by OPA1. Another study using cells isolated from OPA1$^{+/-}$ mice reported mitochondrial respiratory deficiency and selective loss of complex IV caused by decreased OPA1 levels.[45] Taken together, these studies indicate that reduced OPA1 expression may promote mitochondrial dysfunction.

In addition to OPA1 synthesis, there has been a growing interest in the processing of OPA1 and its effect on mitochondrial dynamics.[46,47] In OPA1 biogenesis, the long form of OPA1 (L-OPA1) can undergo cleavage at two proteolytic cleavage sites, S1 and S2, into two short forms of OPA1 (S-OPA1) by peptidases OMA1 and YME1L residing on the inner membrane.[48–51] Studies suggest that mature OPA1 constitutively undergoes processing at S1 and S2 cleavage sites at steady state[52] and that a homeostatic balance is needed between L-OPA1 and S-OPA1 forms to maintain normal mitochondrial morphology.[51] Interestingly, the long and short OPA1 isoforms have little activity individually but functionally complement each other when coexpressed, leading to optimal fusion activity.[51] Moreover, studies suggest that L-OPA1 alone is sufficient to promote fusion, whereas excess cleavage of L-OPA1 into S-OPA1 forms under pathological stress is mostly associated with mitochondrial fission.[22,52–54] Of note, in the ischemia-reperfusion–injured retina, restoration of L-Opa1 level improved mitochondrial morphology and inhibited apoptosis.[55] Interestingly, one of the diabetic animals from the present study exhibited great extent of reduction in L-OPA1 than the rest, but this phenomenon remains under further investigation. These findings suggest that further studies are necessary to investigate the mechanisms by which OPA1 downregulation occurs, and whether HG conditions influence OPA1 processing and thereby influence mitochondrial dynamics in the context of diabetic retinopathy.

Although OPA1 plays a critical role in regulating mitochondrial structure, other genes such as MFN2, DRP1, and FIS1, are known to be involved in mitochondrial fission and fusion process. For example, MFN2, a mitochondrial fusion gene, has been found to be decreased in the retinal vessels of diabetic rats[56] and retinas of human eyes with diabetic retinopathy.[57] Furthermore, a study has shown that diabetes promotes hypermethylation of the MFN2 promoter and suppresses MFN2 expression, and that upregulation of MFN2 in HG condition increased mitochondrial fusion and led to the formation of elongated mitochondria.[57] These findings

indicate that mitochondrial dynamics is a complex process, which involves the interaction between fission and fusion events in regulating mitochondrial morphology and functionality under HG condition. The current study provides evidence for the role of HG- or diabetes-induced downregulation of OPA1 level in retinal vascular cells, which can negatively influence mitochondrial dynamics through increased mitochondrial fragmentation, cytochrome c release, and initiation of apoptosis. Therefore further investigation is needed to determine whether targeting abnormal OPA1 downregulation protects against the development of retinal vascular lesions associated with diabetic retinopathy.

Acknowledgments

Supported by NEI, NIH Grant EY027082 (SR).

Disclosure: **D. Kim,** None; **S. Roy,** None

References

1. Fong DS, Aiello L, Gardner TW, et al. Retinopathy in diabetes. *Diabetes Care*. 2004;27(Suppl 1):S84–S87.
2. Wild S, Roglic G, Green A, Sicree R, King H. Global prevalence of diabetes: estimates for the year 2000 and projections for 2030. *Diabetes Care*. 2004;27:1047–1053.
3. Engerman RL. Pathogenesis of diabetic retinopathy. *Diabetes*. 1989;38:1203–1206.
4. Hammes HP, Lin J, Renner O, et al. Pericytes and the pathogenesis of diabetic retinopathy. *Diabetes*. 2002;51:3107–3112.
5. Li W, Yanoff M, Liu X, Ye X. Retinal capillary pericyte apoptosis in early human diabetic retinopathy. *Chin Med J (Engl)*. 1997;110:659–663.
6. Mizutani M, Kern TS, Lorenzi M. Accelerated death of retinal microvascular cells in human and experimental diabetic retinopathy. *The Journal of Clinical Investigation*. 1996;97:2883–2890.
7. Podesta F, Romeo G, Liu WH, et al. Bax is increased in the retina of diabetic subjects and is associated with pericyte apoptosis in vivo and in vitro. *The American Journal of Pathology*. 2000;156:1025–1032.
8. Cunha-Vaz J, Bernardes R. Nonproliferative retinopathy in diabetes type 2. Initial stages and characterization of phenotypes. *Progress in Retinal and Eye Research*. 2005;24:355–377.
9. Oshitari T, Yamamoto S, Hata N, Roy S. Mitochondria- and caspase-dependent cell death pathway involved in neuronal degeneration in diabetic retinopathy. *Br J Ophthalmol*. 2008;92:552–556.
10. Trudeau K, Molina AJ, Guo W, Roy S. High glucose disrupts mitochondrial morphology in retinal endothelial cells: implications for diabetic retinopathy. *Am J Pathol*. 2010;177:447–455.
11. Trudeau K, Molina AJ, Roy S. High glucose induces mitochondrial morphology and metabolic changes in retinal pericytes. *Invest Ophthalmol Vis Sci*. 2011;52:8657–8664.
12. Trudeau K, Muto T, Roy S. Downregulation of mitochondrial connexin 43 by high glucose triggers mitochondrial shape change and cytochrome C release in retinal endothelial cells. *Invest Ophthalmol Vis Sci*. 2012;53:6675–6681.
13. Roy S, Trudeau K, Roy S, Tien T, Barrette KF. Mitochondrial dysfunction and endoplasmic reticulum stress in diabetic retinopathy: mechanistic insights into high glucose-induced retinal cell death. *Curr Clin Pharmacol*. 2013;8:278–284.
14. Tien T, Zhang J, Muto T, Kim D, Sarthy VP, Roy S. High glucose induces mitochondrial dysfunction in retinal muller cells: implications for diabetic retinopathy. *Invest Ophthalmol Vis Sci*. 2017;58:2915–2921.
15. Roy S, Kim D, Sankaramoorthy A. Mitochondrial structural changes in the pathogenesis of diabetic retinopathy. *J Clin Med*. 2019;8:1363.
16. Arnoult D, Grodet A, Lee YJ, Estaquier J, Blackstone C. Release of OPA1 during apoptosis participates in the rapid and complete release of cytochrome c and subsequent mitochondrial fragmentation. *J Biol Chem*. 2005;280:35742–35750.
17. Davies VJ, Hollins AJ, Piechota MJ, et al. Opa1 deficiency in a mouse model of autosomal dominant optic atrophy impairs mitochondrial morphology, optic nerve structure and visual function. *Hum Mol Genet*. 2007;16:1307–1318.
18. Frezza C, Cipolat S, Martins de Brito O, et al. OPA1 controls apoptotic cristae remodeling independently from mitochondrial fusion. *Cell*. 2006;126:177–189.
19. Olichon A, Baricault L, Gas N, et al. Loss of OPA1 perturbates the mitochondrial inner membrane structure and integrity, leading to cytochrome c release and apoptosis. *J Biol Chem*. 2003;278:7743–7746.
20. Galloway CA, Yoon Y. Mitochondrial dynamics in diabetic cardiomyopathy. *Antioxid Redox Signal*. 2015;22:1545–1562.
21. Olichon A, Guillou E, Delettre C, et al. Mitochondrial dynamics and disease, OPA1. *Biochim Biophys Acta*. 2006;1763:500–509.
22. Ishihara N, Fujita Y, Oka T, Mihara K. Regulation of mitochondrial morphology through proteolytic cleavage of OPA1. *EMBO J*. 2006;25:2966–2977.
23. Song Z, Ghochani M, McCaffery JM, Frey TG, Chan DC. Mitofusins and OPA1 mediate sequential steps in mitochondrial membrane fusion. *Mol Biol Cell*. 2009;20:3525–3532.
24. Cipolat S, Martins de Brito O, Dal Zilio B, Scorrano L. OPA1 requires mitofusin 1 to promote mitochondrial fusion. *Proc Natl Acad Sci USA*. 2004;101:15927–15932.
25. Lee H, Yoon Y. Mitochondrial fission and fusion. *Biochem Soc Trans*. 2016;44:1725–1735.
26. van der Bliek AM, Shen Q, Kawajiri S. Mechanisms of mitochondrial fission and fusion. *Cold Spring Harb Perspect Biol*. 2013;5:a011072.
27. Griparic L, van der Wel NN, Orozco IJ, Peters PJ, van der Bliek AM. Loss of the intermembrane space protein Mgm1/OPA1 induces swelling and localized constrictions along the lengths of mitochondria. *J Biol Chem*. 2004;279:18792–18798.
28. MacVicar T, Langer T. OPA1 processing in cell death and disease—the long and short of it. *J Cell Sci*. 2016;129:2297–2306.
29. Makino A, Scott BT, Dillmann WH. Mitochondrial fragmentation and superoxide anion production in coronary endothelial cells from a mouse model of type 1 diabetes. *Diabetologia*. 2010;53:1783–1794.
30. Parra V, Verdejo HE, Iglewski M, et al. Insulin stimulates mitochondrial fusion and function in cardiomyocytes via the Akt-mTOR-NFkappaB-Opa-1 signaling pathway. *Diabetes*. 2014;63:75–88.
31. Pereira RO, Tadinada SM, Zasadny FM, et al. OPA1 deficiency promotes secretion of FGF21 from muscle that prevents obesity and insulin resistance. *EMBO J*. 2017;36:2126–2145.
32. Rodriguez-Nuevo A, Diaz-Ramos A, Noguera E, et al. Mitochondrial DNA and TLR9 drive muscle inflammation upon Opa1 deficiency. *EMBO J*. 2018;37:e96553.
33. Shenouda SM, Widlansky ME, Chen K, et al. Altered mitochondrial dynamics contributes to endothelial dysfunction in diabetes mellitus. *Circulation*. 2011;124:444–453.

34. Tezze C, Romanello V, Desbats MA, et al. Age-associated loss of OPA1 in muscle impacts muscle mass, metabolic homeostasis, systemic inflammation, and epithelial senescence. *Cell Metab*. 2017;25:1374–1389.e1376.
35. Wang X, Li H, Zheng A, et al. Mitochondrial dysfunction-associated OPA1 cleavage contributes to muscle degeneration: preventative effect of hydroxytyrosol acetate. *Cell Death Dis*. 2014;5:e1521.
36. Zhang Z, Wakabayashi N, Wakabayashi J, et al. The dynamin-related GTPase Opa1 is required for glucose-stimulated ATP production in pancreatic beta cells. *Mol Biol Cell*. 2011;22:2235–2245.
37. Chronopoulos A, Trudeau K, Roy S, Huang H, Vinores SA, Roy S. High glucose-induced altered basement membrane composition and structure increases trans-endothelial permeability: implications for diabetic retinopathy. *Curr Eye Res*. 2011;36:747–753.
38. Towbin H, Staehelin T, Gordon J. Electrophoretic transfer of proteins from polyacrylamide gels to nitrocellulose sheets: procedure and some applications. *Proc Natl Acad Sci USA*. 1979;76:4350–4354.
39. De Vos KJ, Allan VJ, Grierson AJ, Sheetz MP. Mitochondrial function and actin regulate dynamin-related protein 1-dependent mitochondrial fission. *Curr Biol*. 2005;15:678–683.
40. Koopman WJ, Verkaart S, Visch HJ, et al. Inhibition of complex I of the electron transport chain causes O2–mediated mitochondrial outgrowth. *Am J Physiol Cell Physiol*. 2005;288:C1440–C1450.
41. Seervi M, Joseph J, Sobhan PK, Bhavya BC, Santhoshkumar TR. Essential requirement of cytochrome c release for caspase activation by procaspase-activating compound defined by cellular models. *Cell Death Dis*. 2011;2:e207.
42. Nakajima YI, Kuranaga E. Caspase-dependent non-apoptotic processes in development. *Cell Death Differ*. 2017;24:1422–1430.
43. Liu Y, Minze LJ, Mumma L, Li XC, Ghobrial RM, Kloc M. Mouse macrophage polarity and ROCK1 activity depend on RhoA and non-apoptotic Caspase 3. *Exp Cell Res*. 2016;341:225–236.
44. Chen L, Liu T, Tran A, et al. OPA1 mutation and late-onset cardiomyopathy: mitochondrial dysfunction and mtDNA instability. *J Am Heart Assoc*. 2012;1:e003012.
45. Kushnareva Y, Seong Y, Andreyev AY, et al. Mitochondrial dysfunction in an Opa1(Q285STOP) mouse model of dominant optic atrophy results from Opa1 haploinsufficiency. *Cell Death Dis*. 2016;7:e2309.
46. Quiros PM, Langer T, Lopez-Otin C. New roles for mitochondrial proteases in health, ageing and disease. *Nat Rev Mol Cell Biol*. 2015;16:345–359.
47. Roy M, Reddy PH, Iijima M, Sesaki H. Mitochondrial division and fusion in metabolism. *Curr Opin Cell Biol*. 2015;33:111–118.
48. Ehses S, Raschke I, Mancuso G, et al. Regulation of OPA1 processing and mitochondrial fusion by m-AAA protease isoenzymes and OMA1. *J Cell Biol*. 2009;187:1023–1036.
49. Griparic L, Kanazawa T, van der Bliek AM. Regulation of the mitochondrial dynamin-like protein Opa1 by proteolytic cleavage. *J Cell Biol*. 2007;178:757–764.
50. Head B, Griparic L, Amiri M, Gandre-Babbe S, van der Bliek AM. Inducible proteolytic inactivation of OPA1 mediated by the OMA1 protease in mammalian cells. *J Cell Biol*. 2009;187:959–966.
51. Song Z, Chen H, Fiket M, Alexander C, Chan DC. OPA1 processing controls mitochondrial fusion and is regulated by mRNA splicing, membrane potential, and Yme1L. *J Cell Biol*. 2007;178:749–755.
52. Anand R, Wai T, Baker MJ, et al. The i-AAA protease YME1L and OMA1 cleave OPA1 to balance mitochondrial fusion and fission. *J Cell Biol*. 2014;204:919–929.
53. Tondera D, Grandemange S, Jourdain A, et al. SLP-2 is required for stress-induced mitochondrial hyperfusion. *EMBO J*. 2009;28:1589–1600.
54. Wai T, Garcia-Prieto J, Baker MJ, et al. Imbalanced OPA1 processing and mitochondrial fragmentation cause heart failure in mice. *Science*. 2015;350:aad0116.
55. Sun Y, Xue W, Song Z, Huang K, Zheng L. Restoration of Opa1-long isoform inhibits retinal injury-induced neurodegeneration. *J Mol Med (Berl)*. 2016;94:335–346.
56. Zhong Q, Kowluru RA. Diabetic retinopathy and damage to mitochondrial structure and transport machinery. *Invest Ophthalmol Vis Sci*. 2011;52:8739–8746.
57. Duraisamy AJ, Mohammad G, Kowluru RA. Mitochondrial fusion and maintenance of mitochondrial homeostasis in diabetic retinopathy. *Biochim Biophys Acta Mol Basis Dis*. 2019;1865:1617–1626.

Investigative Ophthalmology & Visual Science